The 3-RPS Manipulator Can Have Non-Singular Assembly-Mode Changes

Manfred Husty, Josef Schadlbauer, Stéphane Caro and Philippe Wenger

Abstract Recently a complete kinematic description of the 3-RPS parallel manipulator was obtained using algebraic constraint equations. It turned out that the workspace decomposes into two components describing two kinematically different operation modes and that self-motions of this manipulator in both operation are possible. In this paper for the first time it is shown that this manipulator has the property of non singular assembly mode change.

Keywords 3-RPS-manipulator · Singularities · Assembly mode change

1 Introduction

Non-singular assembly mode change has been discussed a lot for parallel manipulators since Innocenti and Parenti-Castelli [1] showed examples of such a behavior. Especially planar 3-RPR parallel manipulators were extensively investigated with respect to non-singular assembly mode change (see e.g. [2] and [3]). In [4] it was shown, that every generic planar 3-RPR has two aspects, meaning that the singularity surface divides the workspace into two parts and therefore non-singular assembly

M. Husty · J. Schadlbauer
Institute for Basic Sciences in Engineering, Unit for Geometry and CAD,
University of Innsbruck, Innsbruck, Austria
e-mail: manfred.husty@uibk.ac.at

J. Schadlbauer
e-mail: josef.schadlbauer@uibk.ac.at

S. Caro · P. Wenger (✉)
Institut de Recherche en Communications et Cybernétique de Nantes,
Nantes, France
e-mail: stephane.caro@irccyn.ec-nantes.fr

P. Wenger
e-mail: philippe.wenger@irccyn.ec-nantes.fr

mode change is always possible. To the best of the knowledge of the authors singularity free assembly mode change has never been shown explicitly for spatial lower mobility parallel manipulators. It is the motivation to demonstrate this behavior for such a manipulator. One of the best investigated designs of lower mobility parallel manipulators is the 3-RPS manipulator introduced by Hunt [5]. This manipulator is simple enough to make this task feasible.

A 3-RPS manipulator is a three degree of freedom (DOF) parallel manipulator. It consists of an equilateral triangular fixed platform and a similar moving platform connected by three identical RPS legs. The first joint (R-joint) is connected to the base and the last joint (S-joint) is connected to the moving platform (see Fig. 1). The legs are extensible, changing lengths via prismatic joints (P-joints), thereby moving the platform with three highly coupled DOFs. In the past few years the 3-RPS obtained a lot of attention in the kinematics community, see e.g. [6].

In [7] an overview of existing results up to the year 2008 can be found. Local analysis, mostly using screw theory was performed in most of the existing investigations especially in [8] and [9]. More recently in [10], using an algebraic description of the manipulator, together with *Study*'s kinematic mapping, a complete characterization of the forward kinematics, the operation modes, the singular poses and the transitions between the operation modes was given. It turned out that the manipulator has two kinematically different operation modes. The first one is characterized by finite π-screws. Axes of these screws are tilted with respect to the base and the translation distance depends on the chosen axis. The second mode has horizontal screw axes with rotation angle and translation distance depending on the chosen axis. Note, that this characterization refers to finite screws and not instantaneous screws. The singularities in both operation modes were derived in the kinematic image space as well as in the joint space. In joint space the singularity surfaces are of degree 24 and it was shown that for input joint combinations fulfilling an eight order polynomial transition from one operation mode to the other is possible. In [11] it was shown, that the manipulator can perform a spherical and "butterfly" self-motion for special leg lengths.

In this paper an example of singularity free assembly mode change will be given. To prove this property a singularity free path will be constructed that moves the manipulator around a cusp in a slice of its workspace.

The paper is organized as follows: In Sect. 2 a description of the architecture of the 3-RPS is given and the set of constraint equations is recalled. Section 3 introduces a method to construct a nonsingular assembly mode change path for this manipulator.

2 Robot Design

With respect to Fig. 1 we consider the 3-RPS parallel manipulator with the following architecture: The base of the 3-RPS consists of an equilateral triangle with vertices $\mathbf{A}_1$, $\mathbf{A}_2$ and $\mathbf{A}_3$ and circumradius h_1. The origin of the fixed frame Σ_0 coincides with the circumcenter of the triangle $\mathbf{A}_1$, $\mathbf{A}_2$ and $\mathbf{A}_3$. The yz-plane of Σ_0 is defined

Fig. 1 Design of the 3-RPS
parallel robot
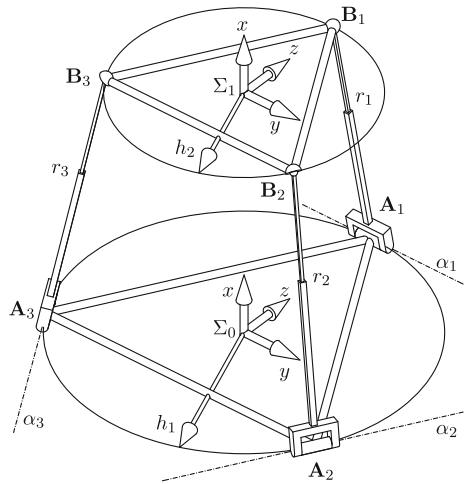
by the plane $\mathbf{A}_1$, $\mathbf{A}_2$, $\mathbf{A}_3$. Finally, $\mathbf{A}_1$ lies on the z-axis of Σ_0. In the platform there
is another equilateral triangle with vertices $\mathbf{B}_1$, $\mathbf{B}_2$ and $\mathbf{B}_3$ and circumradius h_2.
The circumcenter of the triangle $\mathbf{B}_1$, $\mathbf{B}_2$ and $\mathbf{B}_3$ lies in the origin of Σ_1, which is
the moving frame. Again, the plane defined by $\mathbf{B}_1$, $\mathbf{B}_2$ and $\mathbf{B}_3$ coincides with the
yz-plane of Σ_1 and $\mathbf{B}_1$ lies on the z-axis of Σ_1.

The two design parameters h_1 and h_2 are taken to be strictly positive numbers.
Now each pair of vertices $\mathbf{A}_i$, $\mathbf{B}_i$ ($i = 1, \ldots, 3$) is connected by a limb, with a
rotational joint at $\mathbf{A}_i$ and a spherical joint at $\mathbf{B}_i$. The length of each limb is denoted
by r_i and is adjusted via an actuated prismatic joint. The axes α_i of the rotational
joints at $\mathbf{A}_i$ are tangent to the circumcircle and therefore lie within the yz-plane
of Σ_0. Overall we have five parameters, namely h_1, h_2, r_1, r_2 and r_3. While h_1
and h_2 determine the design of the manipulator, the parameters r_1, r_2 and r_3 are
joint parameters, which determine the motion of the robot. We can consider the
joint parameters to be like design parameters when they are assigned with specific
leg lengths r_i. In some computations the leg lengths r_i will be replaced with their
squares which then will be denoted by R_i. Deriving the constraint equations is one
essential step in solving the kinematics of a manipulator. To compute these equations
which describe the motion capability, the direct kinematics and also the singularities
of the manipulator, we use the *Study*-parameterization of the motion group $SE(3)$.
The vertices of the base triangle and the platform triangle in Σ_0 resp. Σ_1 are

$$\mathbf{A}_1 = (1, 0, 0, h_1), \quad \mathbf{A}_2 = (1, 0, \sqrt{3}h_1/2, -h_1/2), \quad \mathbf{A}_3 = (1, 0, -\sqrt{3}h_1/2, -h_1/2)$$

$$\mathbf{b}_1 = (1, 0, 0, h_2), \quad \mathbf{b}_2 = (1, 0, \sqrt{3}h_2/2, -h_2/2), \quad \mathbf{b}_3 = (1, 0, -\sqrt{3}h_2/2, -h_2/2)$$

thereby using projective coordinates with the homogenizing coordinate in first place.
To avoid confusion coordinates with respect to Σ_0 are written in capital letters and
those with respect to Σ_1 are in lower case. To obtain the coordinates $\mathbf{B}_1$, $\mathbf{B}_2$ and $\mathbf{B}_3$

of $\mathbf{b}_1$, $\mathbf{b}_2$ and $\mathbf{b}_3$ with respect to Σ_0 a coordinate transformation has to be applied. To describe this coordinate transformation we use *Study's* parameterization of a spatial Euclidean transformation matrix $\mathbf{M} \in SE(3)$ (for detailed information on this approach see [12]).

$$\mathbf{M} = \begin{pmatrix} x_0^2 + x_1^2 + x_2^2 + x_3^2 & \mathbf{0}^\top \\ \mathbf{M}_T & \mathbf{M}_R \end{pmatrix}, \quad \mathbf{M}_T = \begin{pmatrix} 2(-x_0 y_1 + x_1 y_0 - x_2 y_3 + x_3 y_2) \\ 2(-x_0 y_2 + x_1 y_3 + x_2 y_0 - x_3 y_1) \\ 2(-x_0 y_3 - x_1 y_2 + x_2 y_1 + x_3 y_0) \end{pmatrix}$$

$$\mathbf{M}_R = \begin{pmatrix} x_0^2 + x_1^2 - x_2^2 - x_3^2 & 2(x_1 x_2 - x_0 x_3) & 2(x_1 x_3 + x_0 x_2) \\ 2(x_1 x_2 + x_0 x_3) & x_0^2 - x_1^2 + x_2^2 - x_3^2 & 2(x_2 x_3 - x_0 x_1) \\ 2(x_1 x_3 - x_0 x_2) & 2(x_2 x_3 + x_0 x_1) & x_0^2 - x_1^2 - x_2^2 + x_3^2 \end{pmatrix}$$

The vector $\mathbf{M}_T$ represents the translational part and $\mathbf{M}_R$ represents the rotational part of the transformation $\mathbf{M}$. The parameters $x_0, x_1, x_2, x_3, y_0, y_1, y_2, y_3$ which appear in the matrix $\mathbf{M}$ are called *Study*-parameters of the transformation $\mathbf{M}$. The mapping

$$\kappa : SE(3) \to P \in \mathbb{P}^7 \tag{1}$$

$$\mathbf{M}(x_i, y_i) \mapsto (x_0 : x_1 : x_2 : x_3 : y_0 : y_1 : y_2 : y_3)^T \neq (0 : 0 : 0 : 0 : 0 : 0 : 0 : 0)^T$$

is called *kinematic mapping* and maps each Euclidean displacement of $SE(3)$ to a point P on a quadric $S_6^2 \subset \mathbb{P}^7$. In this way, every projective point $(x_0 : x_1 : x_2 : x_3 : y_0 : y_1 : y_2 : y_3) \in \mathbb{P}^7$ represents a spatial Euclidean transformation, if it fulfills the following equation $S_6^2 : x_0 y_0 + x_1 y_1 + x_2 y_2 + x_3 y_3 = 0$ and inequality: $x_0^2 + x_1^2 + x_2^2 + x_3^2 \neq 0$ (see [12]).

The coordinates of $\mathbf{b}_i$ with respect to Σ_0 are obtained by:

$$\mathbf{B}_i = \mathbf{M} \cdot \mathbf{b}_i, \quad i = 1, \dots, 3.$$

Now, as the coordinates of all vertices are given in terms of the transformation parameters $x_0, x_1, x_2, x_3, y_0, y_1, y_2, y_3$ and the design constants, we obtain constraint equations by examining the geometry of the manipulator more closely. First of all the limb connecting $\mathbf{A}_i$ and $\mathbf{B}_i$ has to be orthogonal to the corresponding rotational axis α_i. That means, the scalar product of the vector connecting $\mathbf{A}_i \mathbf{B}_i$ and the direction of α_i vanishes. After computing this product, removing the common denominator $(x_0^2 + x_1^2 + x_2^2 + x_3^2)$ and performing some elementary simplifications the following equations are obtained:

$$g_1 : x_0 x_1 = 0$$
$$g_2 : h_2 x_2^2 - h_2 x_3^2 - 2x_0 y_3 - 2x_1 y_2 + 2x_2 y_1 + 2x_3 y_0 = 0 \tag{2}$$
$$g_3 : 2h_2 x_0 x_1 + h_2 x_2 x_3 - x_0 y_2 + x_1 y_3 + x_2 y_0 - x_3 y_1 = 0.$$

This set of equations is augmented by three leg length conditions:

$$g_4 : (h_1 - h_2)^2 x_0^2 + (h_1 + h_2)^2 x_1^2 + (h_1 + h_2)^2 x_2^2 + (h_1 - h_2)^2 x_3^2 + 4(h_1 - h_2)x_0 y_3 + 4(h_1 + h_2)x_1 y_2$$
$$- 4(h_1 + h_2)x_2 y_1 - 4(h_1 - h_2)x_3 y_0 + 4(y_0^2 + y_1^2 + y_2^2 + y_3^2) - (x_0^2 + x_1^2 + x_2^2 + x_3^2)R_1 = 0$$
$$g_5 : (h_1 - h_2)^2 x_0^2 + (h_1 + h_2)^2 x_1^2 + (h_1^2 + h_2^2 - h_1 h_2)x_2^2 + (h_1^2 + h_2^2 + h_1 h_2)x_3^2 - 2(h_1$$
$$- h_2)x_0 y_3 - 2(h_1 + h_2)x_1 y_2 + 2(h_1 + h_2)x_2 y_1 + 2(h_1 - h_2)x_3 y_0 - 2\sqrt{3}(h_1$$
$$- h_2)x_0 y_2 + 2\sqrt{3}(h_1 + h_2)x_1 y_3 + 2\sqrt{3}(h_1 - h_2)x_2 y_0 - 2\sqrt{3}(h_1 + h_2)x_3 y_1$$
$$- 2\sqrt{3}h_1 h_2 x_2 x_3 + 4(y_0^2 + y_1^2 + y_2^2 + y_3^2) - (x_0^2 + x_1^2 + x_2^2 + x_3^2)R_2 = 0$$
$$g_6 : (h_1 - h_2)^2 x_0^2 + (h_1 + h_2)^2 x_1^2 + (h_1^2 + h_2^2 - h_1 h_2)x_2^2 + (h_1^2 + h_2^2 + h_1 h_2)x_3^2 - 2(h_1$$
$$- h_2)x_0 y_3 - 2(h_1 + h_2)x_1 y_2 + 2(h_1 + h_2)x_2 y_1 + 2(h_1 - h_2)x_3 y_0 + 2\sqrt{3}(h_1$$
$$- h_2)x_0 y_2 - 2\sqrt{3}(h_1 + h_2)x_1 y_3 - 2\sqrt{3}(h_1 - h_2)x_2 y_0 + 2\sqrt{3}(h_1 + h_2)x_3 y_1$$
$$+ 2\sqrt{3}h_1 h_2 x_2 x_3 + 4(y_0^2 + y_1^2 + y_2^2 + y_3^2) - (x_0^2 + x_1^2 + x_2^2 + x_3^2)R_3 = 0.$$

A detailed explanation of how this set of equations is derived is left out for sake of lack of space but can be found in [10]. To complete the system, we add the Study-equation (g_7), because all the solutions have to be within the Study-Quadric and a normalizing condition (g_8).

$$g_7 : x_0 y_0 + x_1 y_1 + x_2 y_2 + x_3 y_3 = 0, \quad g_8 : x_0^2 + x_1^2 + x_2^2 + x_3^2 = 1 \quad (3)$$

It is emphasized that R_i in equations g_4, g_5, g_6 denote the squares of the input parameters (leg lengths). The set of equations describing a general 3-RPS manipulator forms the ideal

$$\mathcal{I} = \langle g_1, g_2, g_3, g_4, g_5, g_6, g_7, g_8 \rangle \quad (4)$$

From the first equation in this set it is obvious, that this ideal consists of two components $\mathcal{K}_1 = \langle x_0, g_2, g_3, g_4, g_5, g_6, g_7, g_8 \rangle$ and $\mathcal{K}_2 = \langle x_1, g_2, g_3, g_4, g_5, g_6, g_7, g_8 \rangle$. It was shown in [10] that these two components can be treated separately to compute the direct kinematics and all singularities of this manipulator. Therefore the same can be done for computing non singular assembly mode change of this manipulator type.

3 Non-Singular Assembly Mode Change

The main idea in [4] to prove the non-singular assembly mode change behavior is the representation of the singularity surface in the three dimensional kinematic image space, where the two aspects of the singularity surface can be visualized and singularity free assembly mode changing paths can be constructed easily. A similar method was used in [13] and [14] to prove the assembly mode changing property for spherical 3-RPR parallel manipulators.
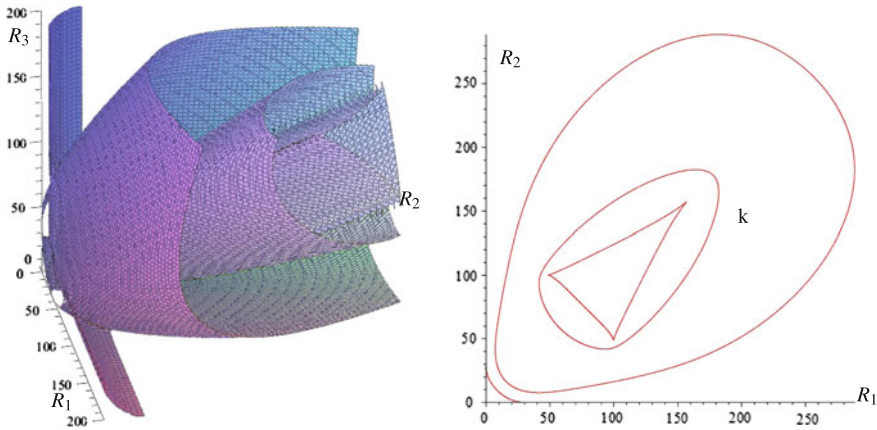
Fig. 2 Singularity surface S in joint space $h_1 = 1, h_2 = 2$ Slice through S at $R_3 = 100$

The same method as in planar and spherical cases cannot be used for a 3-dof spatial manipulator. It is not possible to derive the singularity surface in a 3-dim kinematic image space and construct singularity free paths, because the singularity surface is contained in the 7-dim kinematic image space of spatial displacements and therefore difficult to handle. In the following a new method is presented to overcome these difficulties and to prove that non-singular assembly mode change is also possible in case of a 3-RPS parallel manipulator.

The two governing ideals $\mathcal{K}_1$ and $\mathcal{K}_2$ which describe the motion capabilities of the manipulator, are treated separately. It was already shown in [10] that the singularity surface for each component can be computed in the kinematic image space and in the joint space.

The singularity surface in the joint space, by using the leg lengths r_i, $i = 1 \ldots 3$ as coordinates, has degree 24. A closer inspection shows that the variables of the singularity surface in joint space have only even powers. Therefore it makes sense to use the squares of the leg lengths as new coordinates. After the substitution $R_i = r_i^2$ the resulting singularity surface S has only degree 12. A part of S for the parameters $h_1 = 1, h_2 = 2$ is displayed in (Fig. 2).

Next the univariate polynomial of one ideal $\mathcal{K}_i$ in one of the Study parameters is computed. This can be done without specifying the leg length parameters R_i. For this purpose an ordered Groebner basis of the ideal e.g. $\mathcal{K}_1$ is computed and this yields a univariate polynomial F of degree eight in one variable (e.g. x_2) having only even powers

$$F : a_0 x_2^8 + b_0 x_2^6 + c_0 x_2^4 + d_0 x_2^2 + f_0 = 0, \tag{5}$$

where a_0, b_0, c_0, d_0, f_0 are polynomials in the input parameters R_1, R_2, R_3 and the design parameter h_2 (without loss of generality $h_1 = 1$ has been set). In the following we will take x_2 as paradigmatic example for the used Study parameter. Note that

x_2 could be replaced by any other Study parameter if the univariate polynomial had been computed in this other parameter.

Then a slice through the singularity surface is taken by setting one joint parameter constant $R_i = c$. Figure 2 shows an example of such a slice; the intersection curve is denoted k (the chosen joint parameters in the example are $R_1 = R_2 = 120$, $R_3 = 100$). The constant value c is also substituted into F. The result is a polynomial F_p in two joint parameters and one Study parameter. This polynomial can be viewed as level-set in the Study parameter x_2. The graph of this level-set is a surface

$$F_p(R_j, R_k, v) = 0, \ \ j, k \in \{1, 2, 3\}, \ j, k \neq i$$

of degree 4 in the square of the Study parameter $v := x_2^2$. We display it in the same coordinate system as the slice and extend the intersection curve k also to a level set. This level-set is trivial, because it is only the cylinder S_L above the intersection curve. It is interesting to note, that S_L is tangent to F_p. The curve of tangency is exactly the set of singularities of the manipulator, which belong to values of x_2 on F_p. The cusps on the inner part of k indicate that the surface F_P folds back and a singularity free assembly mode changing path can be constructed. The interior of the inner most part of the curve k is a four solutions region of the direct kinematics and outside of this region and inside of the outermost part of k there are two solutions. Now the methodology used in [3] can be applied. We construct in the plane $R_i = c$ a path around the cusp starting at the point S in the interior of the three cusp curve and ending at the point E which is coincident with S but belonging to another solution of the direct kinematics (Fig. 3, lower picture). This path is projected orthogonally in the direction of the v coordinate onto the surface F_p. And in this projection one can see that the level set folds such that S and E are the same points in the slicing plane but belong to different solutions of the direct kinematics. This projection is the computationally most complicated part, because the path, which consists of three line segments in the plane $R_i = const.$, parameterized by a parameter t must be substituted into the polynomial F. The result is a polynomial of degree four in v and degree 8 in t, which must be solved for v. This yields four v coordinate functions, corresponding to four curves which project onto the given three line segment curve in the plane $R_i = c$. Not all four curves will be real in the considered interval. Figure 4 shows that this algorithm is computationally feasible. One can see how the projected curve b runs on the surface F_p. The red wireframe surface is S_L.

In a last step one has to prove that the curve b does not intersect the singularity curve on F. This can be done numerically and is visualized in a classical two view orthogonal projection. The top view is the plane $R_i = c$ (Fig. 3 lower picture). For the front view we take R_j, v as coordinates (Fig. 3 upper picture). The singularity curve on F_p in the top view is the curve k'. The three segment curve was designed such that it runs around the cusp of k'. We have to show that the two apparent intersection points P_1', P_2' in the top view are no intersection points of the curves k and b in space. It can be computed easily that the two apparent intersection points P_1', P_2' are not on the curve k'' in the front view. Graphically this is also shown in Fig. 3. Note that the top view of the singularity curve is computed as the resultant of S_L and F_p with
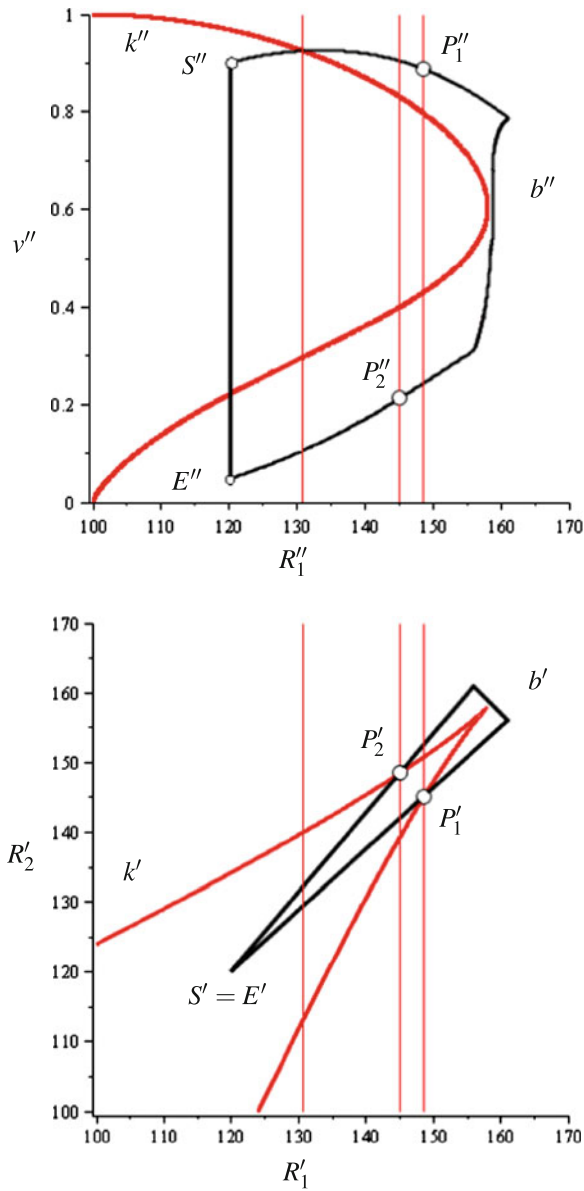
Fig. 3 Singularity curve on F in *front view* and *top view*

respect to the coordinate which is missing in the top view. The same arguments were used to show that the apparent intersection point between the two curves in the front view is no intersection point of the two curves. This proves that the constructed curve connects the two solutions of the direct kinematics without crossing a singularity.
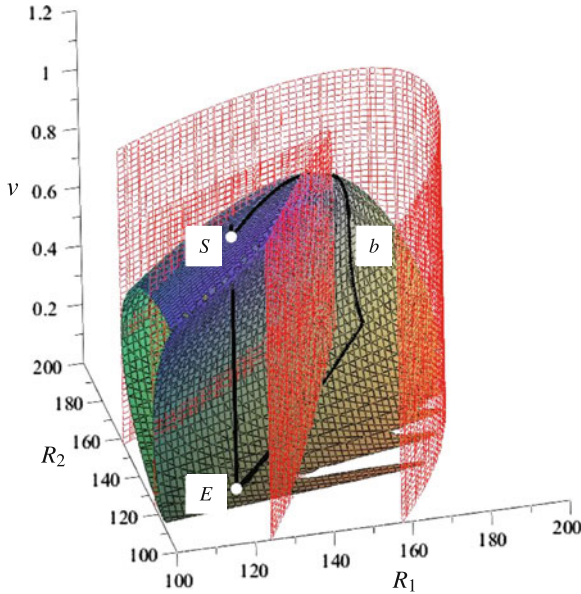
Fig. 4 3-D view of the level-set F singularity levelset S_L and constructed assembly changing curve

4 Conclusion

By constructing a complete example it was shown for the first time that a 3-RPS parallel mechanism allows non-singular assembly mode change. To prove this feature a level set was used and an assembly-mode changing path on the graph of this level set was constructed.

References

1. Innocenti, C., Parenti-Castelli, V.: Singularity-free evolution from one configuration to another in serial and fully-parallel manipulators. J. Mech. Des. **120**, 73–79 (1998)
2. McAree, P.R., Daniel, R.W.: An explanation of never-special assembly changing motions for 33 parallel manipulators. Int. J. Rob. Res. **18**6, 556–574 (1999)
3. Zein, M., Wenger, P., Chablat, D.: Non-singular assembly-mode changing motions for 3-rpr parallel manipulators. Mech. Mach. Theory **43**4, 391–524 (2008)
4. Husty, M.L.: Non-singular assembly mode change in 3-RPR-parallel manipulators. In: Kecskeméthy, A., Müller, A. (eds.) Computational Kinematics, pp. 51–60. Springer, Berlin (2009)
5. Hunt, K.H.: Structural kinematics of in-parallel-actuated robot-arms. Trans. ASME J. Mech. Transm. Autom. Des. **105**, 705–712 (1983)
6. Tsai, L.-W.: Robot Analysis. Wiley, New York (1999)

7. Gallardo, J., Orozco, H., Rico, J., Aguilar, C., Perez, L.: Acceleration analysis of 3-RPS parallel manipulators by means of screw theory. In: Ryu, J.-H. (ed.) Parallel Manipulators, New Developments. I-Tech Education and Publishing, Vienna (2008)
8. Huang, Z., Wang, J., Fang, Y.: Analysis of instantaneous motions of deficient-rank 3-RPS parallel manipulators. Mech. Mach. Theory **37**, 229–240 (2002)
9. Basu, D., Ghosal, A.: Singularity analysis of platform-type multi-loop spatial mechanisms. Mech. Mach. Theory **32**, 375–389 (2002)
10. Schadlbauer, J., Husty, M.-L.: A complete analysis of the 3-RPS manipulator. In: Bandyopadhyay, S., Kumar, G.S., Ramu, P. (eds.) Machines and Mechanisms, pp. 410–419. Narosa Publishing House, New Delhi (2011)
11. Schadlbauer, J., Husty, M., Wenger, P., Caro, S.: Self-motions of 3-RPS manipulators. Front. Mech. Eng. **8**(1), 62–69 (2013)
12. Husty, M.L., Pfurner, M., Schröcker, H.-P., Brunnthaler, K.: Algebraic methods in mechanism analysis and synthesis. Robotica **25**(6), 661–675 (2007)
13. Urizar, M., Husty, M.-L.: Assembly mode change of spherical 3-RPR parallel manipulator. Proceedings of MUSME **2011**, 1–16 (2011)
14. Urizar, M., Husty, M.: Assembly mode change of spherical 3-RPR parallel manipulator. Mech. Based Des. Struct. Mach. **40**, 487–505 (2012)